Int. j. adv. multidisc. res. stud. 2026; 6(1):1888-1893

Received: 15-12-2025
Accepted: 25-01-2026

International Journal of Advanced Multidisciplinary Research and Studies

ISSN: 2583-049X

Assessment of Elemental and Structural Properties of Quartz (SiO_2) Materials Using X-Ray Fluorescence and X-Ray Diffraction Spectrophotometric Methods

[1] Hassan MS, [2] Hassan UF, [3] Garba IH, [4] Mahmoud AA

[1] Department of Chemical Sciences, Federal University of Kashere, Gombe, Nigeria
[2, 3, 4] Department of Chemistry, Abubakar Tafawa Balewa University, Bauchi, Nigeria

Corresponding Author: **Hassan MS**

Abstract

The aim of the investigation was to carry out assessment of elemental and structural properties of quartz materials using X-ray fluorescence and X-ray diffraction spectrophotometric methods. The objectives of the study were to modify standard analytical methods and to provide analytical/geochemical data which would be a guide to aid future beneficiation of the quartz materials from rocks, particularly for the economic exploration and exploitation of quartz and silicate minerals which had wide range of applications in various industries like solar cells and solar panels, glass, nanoparticles, ceramic and paint industries. The study involved collection of rock samples containing quartz minerals from Kwandonkaya, Magama Gumau and Toro within Toro District of Toro Local Government Area of Bauchi State, Nigeria. The purity analysis of the samples was carried out using X-Ray Fluorescence Spectrophotometric method, while the structural properties was determined using X-Ray Diffraction Spectrophotometric method. The XRF analysis of quartz samples revealed the presence of 68.12 ± 0.08 to 75.63 ± 1.05 % SiO_2, 7.34 ± 0.15 to 8.36 ± 9.20 % Al_2O_3, 1.16 ± 0.09 to 4.33 ± 0.15 % CaO and 0.24 ± 0.06 to 0.60 ± 0.34 % MgO. The quartz materials XRD results showed structural properties such as crystalline size, planes and diffraction angles as well as the associated minerals present such as albite, anorthite, biotite, muscovite and orthoclase.

Keywords: Quartz, Silica, Crystallinity Indices, XRF, FTIR, Beneficiation, Nanoparticles, Solar

1. Introduction

In recent years, the interest in raw materials has increased due to their physicochemical properties and availability. Sand is widely used in industry and nanotechnology (Götze and Mökel, 2012). The sand in its raw state is used in various fields as building materials, thermal energy reservoir medium, waters filtering material and in bricks and ceramic manufacture. Sand also represents the most promising resource of quartz (silicon dioxide) material compared to crystalline hard rocks (Diago *et al*., 2015) [3].

Quartz is one of the most abundant minerals found in the earth's crust (12.00 % of its weight). It is a major component of numerous igneous and sedimentary rocks and is present in impure state in many siliceous rocks. The formula is SiO_2 and is composed of two elements, silicon and oxygen. In its amorphous form SiO_2 is the major constituent in many rocks and sand (Gotze, 2009). The crystalline form of SiO_2 or quartz is relatively abundant in nature, but in highly pure form required for manufacture of quartz crystal units, the supply tends to be small. Silica (SiO_2) naturally exists in three main phases of quartz, tridymite and cristobalite and five minor phases of keatite, coesite, melanophogite, fibrous and faujasite (Hong *et al*., 2009) [8]. Quartz, despite being known as SiO_2 has many varieties. The variations are caused by impurities and not all variations of quartz form crystal. Those varieties that do not form crystals are said to be microcrystalline quartz, a sample made up of microscopic crystals of the parent mineral (in this case, quartz). Among these varieties are agate, chalcedony, flint and jasper. Agate appears as a banded, glass-like mineral that is usually found on the inside of geodes and this comprises of chalcedony and often used as decorative mineral. Agate is often dyed brilliant colours for decorative purposes. Chalcedony is a variety of quartz that is formed by fibrous crystals of quartz merging together and known to be blue, white and brown and it is often seen as a component of agate. The hardness of chalcedony is less than crystalline quartz and its specific gravity varies depending on the distance between crystals. Jasper is a reddish - brown variety of microcrystalline quartz that is generally utilized in jewelry (Lűhrs and Geurtsen, 2009) [9].

Today, high purity quartz has become a vital mineral, with its particular physicochemical properties being employed in a wide range of nanotechnologies such as glass fabrication, optics and microelectronics, semiconductors and telecommunications (Moore, 2005) [11]. Quartz contains silicon, which can be exploited in various fields, including medicine, sensor and bio-sensing, photonics, energy technologies and solar application (Hernandez *et al.,* 2015) [7]. Quartz is characterized as high purity, only when it contains less than 50.00 µg g^{-1} of impurities including structurally bound trace elements (B, Li, Ge, Ti, Fe, Mn, Ca, K, Na and P) in the quartz lattice, but also micro minerals inclusions and entrapped liquids, Ultra-pure quartz is rare in nature and larger deposits thereof even more rare. The few ultra-pure found around the world include some kinds of quartz-rich pegmatite and hydrothermal quartz veins (Műller and Ihlen, 2007) [12].

Crystallinity is found to be helpful in determining the colour alteration in bedded cherts, as there is a relationship between quartz crystallinity index, grain size of quartz and conodont colour alteration index (Teji *et al.,* 2002) [19]. It is well known that natural occurrences like lightning striking quartz sand or sandstones can cause vitreous silica to develop (Saikia *et al*., 2008 a) [17]. It is also recognized as an indicator of crystalline forms of other minerals associated with it. When crystallinity of quartz is at peak, the associated minerals are expected to be well crystalline form. The peak value of crystallinity denotes an ordered state of the minerals, while the least value denotes a disordered state. It is therefore paramount to find quartz's crystallinity rather than the associated minerals (Saikia *et al.,* 2008 a) [17].

2. Materials and Methods

2.1 Description of the Study area

The area is about 60.00 km Southwest of Bauchi capital of Bauchi State, between metric grid coordinates between 500554.37 to 5275574.49 and 1105629.11 to 1133101.25 which corresponds to Latitudes 10 o 00' N to 10 o 15' N and Longitudes 9 o 00' E to 9 o 15' E.

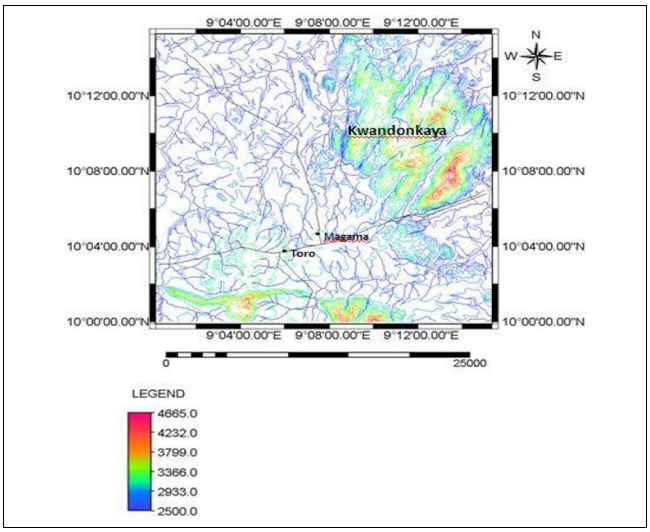

Fig 1: Map of Toro and Environs showing Sampling Locations

2.2 Collection of Rock Samples

Rock samples containing quartz minerals were collected using Hammer from Kwandonkaya, Magama Gumau and Toro**.**

2.2.1 Identification of Rock Samples using Mohs Hardness Scale

The Mohs hardness scale was used as a convenient way to identify the minerals. A mineral's hardness is a measure of its relative resistance to scratching, measured by scratching the mineral against another substance of known hardness on the Mohs Hardness Scale. A smooth unscratched surface of the rock specimen was selected for testing. The rock specimen was held firmly and scratched with the point of an object of known hardness, in this case a sharp quartz (H = 7) crystal was used. The point of the crystal was firmly pressed against the unidentified rock specimen and a feel of definite "bite" into the surface of the rock specimen was not felt, when a finger was used to observe a line etched (scratched) into the surface of the rock specimen. The test was repeated using a sharp point and fresh surface (NIMG, 2020) [13].

2.2.2 Pre-treatment of Rock Samples

The rock samples collected were crushed using Jaw Crusher, sampled with a Riffle box sampler and milled into fine powder (Size: 200 mesh) using Ball Ring Machine Model Number: BV 1111, stored in a polyethylene bag, sealed and labelled appropriately for further analyses (NIMG, 2020) [13].

2.3 Determination of Elemental Compositions of Quartz (SiO_2) Materials using X-Ray Fluorescence Spectrophotometric Method

In X-Ray Fluorescence analysis, high energy x-rays are generated in an x-ray tube by high velocity electron bombardment of metallic anode. These primary x-rays are directed upon the sample to be analyzed. Every element within the sample is excited and emits its own characteristic X-ray spectrum. The intensity of any characteristic X-ray generated is a function of the identity of the element present in the sample. These phenomena provide the basis for a method of chemical analysis. Specific elements within a sample can be identified by the radiation wavelength emitted. The amount of the specific element present can be ascertained by measuring the intensity of its characteristic radiation.

$$2d \, Sin\theta = ג \quad (1)$$

In practice, the various wavelength components of secondary fluorescent radiation emitted by a sample are dispersed by means of a movable diffracting crystal of known inter-atomic spacing, d. The X-ray fluorescence method of analysis has some distinct advantages over conventional wet-chemical methods in many applications. The method is non-destructive towards the sample being analyzed. Its results are not significantly affected by the state of oxidation or chemical combination of the elements analyzed.

The powdered sample was inserted into the X-ray fluorescence spectrophotometer. The X-ray PC was used to select the program for the sample and then identified the sample. The analysis was started, which lasted for about 2-3 min and the result was displayed on the PC screen. Attention was always drawn to the total percentage concentration. Normally, after running the samples, if the total percentage concentration is below 98.00 %, the sample is removed and the monitor runs to standardize the instrument, after which the sample is re-run again (NIMG, 2020) [13].

2.4 Determination of Structural Properties of Quartz Materials using X-Ray Diffraction Spectrophotometric Method

X-ray diffraction is a powerful characterization technique used in the analysis of crystalline solids that exhibit long range order, i.e. when the atomic positions are repeated in a regular fashion. When impacted by light or radiation, a 3-dimensional array of atoms, molecules or ions, cause the light to be diffracted. This behavior is summarized by the expression, nλ = 2d Sinθ (Bragg's Law), where λ = wavelength of radiation used (in our case, Cu [Copper] radiation, λ = 1.5408(Å), d = inter planar spacing within the crystalline solid and θ represents the incident angle between the X-rays and sets of parallel "planes'' in the crystalline solid.

When the X-rays are scattered by the electron clouds of atoms and constructive Interference occurs, the result is recorded as a distinctive powder pattern, plotted as Intensity versus 2θ, where 2θ is the sum of the angle of incidence (θ) and the angle of reflection (θ). Powder patterns for pure phase of mixed powders exhibit peaks at specific values of 2θ and consequently values of d yielding a characteristic "fingerprint" that can be used to identify a crystalline phase or mixture of phases. The values observed for the d spacing are determined by the size and lattice centering of the crystal lattice. The intensities observed are determined by several contributing factors including the identity and positions of the atoms in the lattice, their interaction and absorption of the X-rays. The thermal motion of the scatters as well as the geometry of diffraction experiment can cause peak positions to shift slightly along 2θ (Roper *et al*., 2007) [15].

The width of the peaks is inversely proportional to the crystal size. A thinner peak corresponds to a bigger crystal. A broader peak means that there may be a smaller crystal, defect in the crystalline structure, or that the sample might be amorphous in nature, a solid lacking perfect crystallinity (Doitpoms, 2019) [4].

3. Results and Discussion

3.1 Elemental Composition of Major Oxides in Quartz Materials

The percentage composition of major oxides in quartz materials using X – Ray Fluorescence method are presented in table 1.

Table 1: Percentage Composition of Major Oxides in Quartz Materials using X – Ray Fluorescence Method

	% Composition		
Oxides	**KWK**	**MMG**	**TORO**
SiO_2	75.63 ± 1.05	74.65 ± 1.14	68.12 ± 0.80
Al_2O_3	8.36 ± 0.20	7.34 ± 0.15	7.87 ± 0.69
Fe_2O_3	2.79 ± 0.87	5.08 ± 0.23	8.04 ± 0.54
MnO	0.01 ± 0.00	0.03 ± 0.01	0.22 ± 0.18
Cr_2O_3	N.D.	0.02 ± 0.00	0.02 ± 0.00
TiO_2	0.11 ± 0.02	0.75 ± 0.14	1.29 ± 0.29
P_2O_5	1.59 ± 0.04	1.68 ± 0.13	1.50 ± 0.11
Na_2O	1.52 ± 0.20	1.31 ± 0.08	1.71 ± 0.09
K_2O	7.82 ± 0.05	6.05 ± 0.08	6.04 ± 0.64
CaO	1.16 ± 0.09	2.11 ± 0.02	4.33 ± 0.15
MgO	N.D.	0.24 ± 0.06	0.60 ± 0.34

Values are mean ± standard deviation (n = 3). ND = Not Detected. KWK = Kwandonkaya, and MGM = Magama Gumau

The results of XRF analysis of quartz materials from three different sampling locations in Toro district is shown in Table 1. It reveals that the predominant oxides were SiO_2, Al_2O_3, Fe_2O_3 and K_2O with the percentage ranged of 68.12 ± 0.80 – 75.63 ± 1.05, 7.34 ± 0.15 – 8.36 ± 0.20, 2.79 ± 0.87 – 8.04 ± 0.54 and 6.04 ± 0.64 – 7.82 ± 0.05 % respectively. Obiefuna *et al.* (2018) [14] obtained similar results with SiO_2 content (70.58 %), Al_2O_3 (14.30 %), K_2O (5.44 %), Fe_2O_3 (2.73 %) and CaO (2.62 %). ANOVA results revealed no statistically significant difference between the two groups since ($p > 0.05$).

3.2 X -Ray Diffraction Analysis of Quartz materials

The structural properties and the mineralogical phases of the quartz materials from the three sampling locations within Toro district are presented in Table 2, 3, 4, 2.1, 3.1 and 4.1 respectively.

The range of crystalline sizes of Kwandonkaya quartz materials are 13.80 to 113.60 nm and the mineralogical phases present are quartz, orthoclase muscovite and anorthite as shown in Table 2 and 2.1.

Table 2: Structural Properties of Kwandonkaya Quartz Material

20	(d) Å	hk1	FWHM(deg)	Crystalline Size (mm)	Mineral	Intensity (%)
21.25	21.25	100	0.30	28.40	Quartz	17.72
26.55	3.35	1-1-4	0.17	48.60	Anorthite	29.49
26.87	3.31	101	0.26	32.20	Quartz	88.51
27.83	3.19	20-4	0.62	13.90	Anorthite	79.98
28.09	3.17	002	0.18	45.60	Orthoclase	100. 00
36.80	2.43	110	0.12	67.70	Quartz	46.02
39.80	2.26	102	0.29	30.60	Quartz	6.33
42.72	2.11	200	0.11	78.10	Quartz	5.67
50.36	1.81	0210	0.12	78.10	Muscovite	10.19
50.77	1.79	420	0.08	113.60	Orthoclase	14.35
58.91	1.56	02–8	0.11	86.90	Anorthite	3.96
60.13	1.53	155	0.30	31.80	Muscovite	15.63
68.32	1.37	212	0.73	13.80	Quartz	18.91

2θ° = Diffraction Angle, (d) Å = Interplanar distance, hkl = Miller indices and FWHM = Full Width at Half Maximun

Table 2.1: Results of Qualitative and Quantitative Analysis of Kwandonkaya Quartz Materials

Phase Name	Chemical Formula	Percentage
Quartz	SiO_2	45.00
Orthoclase	$KAlSi_3O_8$	9.00
Muscovite	$KAl_3Si_3O_{10}(OH)_2$	6.40
Anorthite	$CaAl_2Si_2O_8$	39.00

The range of crystalline sizes of Magama Gumau quartz materials are 3.30 to 132.10 nm and the mineralogical phases present are quartz, anorthite, orthoclase and muscovite as shown in Table 3 and 3.1.

Table 3: Structural Properties of Magama Gumau Quartz Materials

2θ°	(d) Å	hkl	FWHM (deg)	Crystallite size (nm)	Mineral	Intensity (%)
20.98	4.23	100	0.12	68.60	Quartz	10.28
22.10	4.01	12-3	0.06	132.10	Anorthite	4.35
23.78	3.74	023	0.08	101.30	Muscovite	2.84
25.60	3.74	11-4	2.50	3.30	Muscovite	12.13
26.74	3.33	101	0.20	40.90	Quartz	100.00
27.55	3.23	002	0.16	52.10	Orthoclase	3.42
39.58	2.27	102	0.17	51.60	Quartz	2.27
42.49	2.12	200	0.16	54.40	Quartz	2.56
45.89	1.97	201	0.16	54.90	Quartz	3.51
50.25	1.81	112	0.17	53.10	Quartz	6.74

55.07	1.66	202	0.17	54.50	Quartz	3.12
60.07	1.53	211	0.13	71.00	Quartz	7.78
60.93	1.51	2010	0.11	87.10	Muscovite	0.66
67.86	1.37	212	0.11	86.50	Quartz	24.72
68.30	1.37	301	0.16	62.20	Quartz	6.07

2θ° = Diffraction Angle, (d) Å = Interplanar distance, hkl = Miller indices and FWHM = Full Width at Half Maximun

Table 3.1: Results of Qualitative and Quantitative Analysis of Magama Gumau Quartz Materials

Phase Name	Chemical Formula	Percentage
Quartz	SiO_2	72.00
Anorthite	$CaAl_2Si_2O_8$	14.20
Orthoclase	$KAlSi_3O_8$	4.00
Muscovite	$K.Al_3Si_3O_{10}(OH)_2$	10.00

The range of crystalline sizes of Toro quartz materials are 24.00 to 95.50 nm and the mineralogical phases present are quartz, biotite albite and anorthite as shown in Table 4 and 4.1.

Table 4: Structural Properties of Toro Quartz Materials

2θ°	(d) Å	hkl	FWHM (deg)	Crystallite size (nm)	Mineral	Intensity (%)
8.90	9.92	001	0.15	55.00	Biotite	47.88
20.94	4.23	100	0.20	42.70	Quartz	11.60
24.13	3.68	11-2	0.35	24.00	Biotite	32.66
24.77	3.59	130	0.17	51.10	Anorthite	23.03
26.72	3.33	101	0.20	41.70	Quartz	100.00
28.03	3.18	002	0.23	36.70	Albite	50.52
28.43	3.13	220	0.15	56.10	Albite	5.35
29.56	3.01	1-31	0.20	41.90	Albite	15.90
39.50	2.27	102	0.12	72.30	Quartz	3.94
40.38	2.23	111	0.09	95.90	Quartz	3.81
41.93	2.15	221	0.09	91.50	Biotite	5.24
42.53	2.12	200	0.23	38.50	Quartz	5.04
50.22	1.81	112	0.29	31.90	Quartz	7.80
50.80	1.79	003	0.19	49.40	Quartz	4.93
59.96	1.54	211	0.26	37.10	Quartz	12.68

2θ° = Diffraction Angle, (d) Å = Interplanar distance, hkl = Miller indices and FWHM = Full Width at Half Maximun

Table 4.1: Results of Qualitative and Quantitative Analysis of Toro Quartz Materials

Phase Name	Chemical Formula	Percentage
Quartz	SiO_2	42.00
Albite	$NaAlSi_3O_2$	16.70
Biotite	$(H.K)_2(Mg.Fe)_2Al_2Si_3O_{12}$	26.00
Anorthite	$CaAl_2Si_2O_8$	15.00

For the purpose of analyzing the crystalline structure of the rocks, XRD technique was used. This technique has been used to analyze the mineralogical composition of the powder materials as well as the phase analysis of the multiphase mixtures. From the values of *d*-spacing as well as the values of 2θ°, it can be confirmed that the possible minerals of the rock samples could be quartz, albite, anorthite, biotite, muscovite and orthoclase and few other minerals, which is in consistent with Sabri (2020) [16]. The main peaks of the XRD data of all quartz materials are related to K-oxide and Fe-oxide. In addition, alumina (Al_2O_3) is also a major trace in all the three quartz material samples of Kwandonkaya, Magama Gumau and Toro. These are in consistent with the XRF data. For example, the main peak of Kwandonkaya quartz material (Table 2) at about 28.09° can be assigned to diffraction of the (0 0 2) plane, which could be for K-oxide. In addition, the XRD pattern of Magama Gumau quartz material (Table 3) exhibits a main plane at about 26.74°, which are corresponding (hkl) to the (101) plane. Finally, the XRD spectrum of Toro quartz material shows a peak at about 26.72°, which corresponding to (101) plane of crystalline phase of silica (quartz), as shown in (Table 9). The crystallinity of the collected quartz material samples from the three different places of Kwandonkaya, Magama Gumau and Toro are proven in the XRD data, as shown in Table 2, 3 and 4. These figures show the similarity in the XRD data in terms of crystallinity for the majority of the quartz material samples, although a minor difference can also be seen in these spectra, which could be due to the origin of the quartz materials.

The average crystalline grain size of the powdered quartz material samples was determined using Debye - Scherrer equation.

$$D = \frac{0.96}{\beta Cos\theta} \quad (2)$$

Where, D, λ, β, θ and 0.96 are the Particle size in nanometre, the Wavelength of the X-ray, the Full Width at Half Maximum, the Peak position and the Scherrer constant respectively.

Using this equation, the crystalline grain size (D) for the collected quartz material samples was found to be as shown in Table 2, 3 and 4.

The XRD pattern of Kwandonkaya quartz material as shown in Table 2 revealed that the diffraction peaks are related to the planes (100), (101), (110), (102), (200) and (212). According to the POWD-12++, (1997) standard pattern, these XRD peaks correspond to quartz with hexagonal crystalline structure and belonging to space group P3121 (152). We observed that the (101) peak has the highest intensity indicating preferred orientation. Further, none of the peaks relating to a plane has fit calcite ($CaCO_3$) compound. The d_{hkl} interplanar spacing has been calculated from the X – ray diffraction profile using the Bragg law:

$$2d_{hkl}Sin\theta = n\lambda \quad (3)$$

Where θ is the diffraction angle, λ is the wavelength of X – rays and n is the order of diffraction. We note that the calculated value of d_{hkl}- spacing (Table 2) matched very well with those of the standard international centre for diffraction data (ICDD). This table also shows that the spacing distances d_{hkl} of 4.17, 3.31 and 2.43 (Å) which is almost the same obtained by Meftah and Mahboub, (2019) [10] and Aderibigbe and Ojuri, (2017) [1] that is 4.43, 3.33 and 2.45 (Å) and hence this affirmed the presence of the α – quartz phase in Kwandonkaya quartz material which is the most stable phase of quartz at room temperature (Beddiaf *et al*, 2015) [2]. Table 8 showed that the value of β was equal to 0.26, that is full width at half maximum (FWHM) of the most intense diffraction peak, usually measured in radian with its corresponding position 2θ = 26.87° meaning the Bragg angle which is very useful when determining the crystalline size D of the quartz material using the Scherrer's formula.

It is clearly shown from Table 3 that the plane (101) with d_{hkl} – spacing of 3.33 in angstrom which corresponds to the

highest peak having a value of 100.00 % followed by the plane (102) with intensity 2.24 % indicating proper orientation. According to POWD – 12 ++, the planes of Magama Gumau quartz also corresponds to hexagonal crystal system with space group P3121 (152), but at diffraction angle (2θ = 39.58) having intensity of 12.13 % meaning Plane (023) it's purely muscovite with Anthorthic as crystal system; space group P – 1 (2). Other diffraction angles such as 22.10, 23.78, 25.60, 27.55 and 60.93 correspond to planes (12-3), (023), (11-4), (002) and (2010) respectively. It is a combination of quartz, Anorthite, Muscovite and Orthoclase minerals.

Diffraction angle of 26.69 Å corresponding to plane (101) has highest peak of 100.00 % as in Magama Gumau quartz indicating proper orientation, followed by plane (102) having diffraction (2θ = 39.52º). All planes of this sample are purely quartz having a hexagonal crystal system with space group P3121 (152). Furthermore, Toro Quartz has a (Å) = b (Å) = 4.90 and c (Å) = 5.40. It is noted that the calculated value of d_{hkl} - spacing (Table 9) matched very well with those of international centre for diffraction data (ICCD), also from this, the spacing distances d_{hkl} of 4.24, 3.33 and 2.45 (Å) which are in conformity with that obtained by Meftah and Mahboub, (2019) [10] and Aderibigbe and Ojuri, (2017) [1] affirmed the presence of the α – quartz phase in Toro sample.

4. Conclusion and Recommendations

4.1 Conclusion

X – Ray Fluorescence and X-Ray Diffraction Spectrophotometric methods were utilized to evaluate the utility and reliability as well as the merits of these analytical methods in the analysis of quartz and associated minerals. Purity, crystallinity, planes and angles were used to characterized the quartz materials. The results can be of benefit to the mining, ceramic, glass, nanoparticles, material science and metallurgical industries.

4.2 Recommendations

Based on the results obtained in this study, the following recommendations were made:

1. There should be result validation using other methods different from XRF and FTIR in the analysis of quartz and other solid minerals.
2. Instrumental techniques such as XRD, SEM, X-ray Photo electron Spectroscopy (XPS) and Attenuated Total Reflectance – FTIR (ATR – FTIR) and Elemental Detector X-ray (EDX) should be used alongside XRF and FTIR to reduce matrix interference.
3. A method for the separation of mineral components of rock sample is necessary for beneficiation of Quartz.
4. Less crystalline rock should be utilized for a good source of (SiO_2) for industrial applications.
5. Proper health monitoring of the residents and employees of the mining area for exposure to heavy metals and disease like silicolisis should be carry out.

5. Acknowledgements

My acknowledgement goes to the Federal University of Kashere, Gombe State and TETFUND for sponsoring my study fellowship and also, the Management and Staff of Nigerian Institute of Mining and Geoscience, Jos for providing me with their Laboratory facilities for this research.

6. References

1. Aderibigbe AD, Ojuri OO. Spectroscopic Characterization of a Nigerian Standard Sand: Igbokoda Sand. International Journal of Geomate. 2017; 12(29):89-98.
2. Beddiaf S, Chihi S, Leghrieb Y. The determination of Some Crystallographic Parameters of Quartz in the Sand Dunes of Quargla, Algeria. Journal of African Earth Science. 2015; 106:129-133.
3. Diago M, Iniesta AC, Delclos T, Shamim T, Calvet N. Characterization of Desert Sand for its Feasible use as Thermal Energy Storage Medium. Energy Procedia. 2015; 75:2113-2118.
4. Doitpoms. TLP Library X-ray Diffraction Techniques-Relationship between Crystalline structure and X-ray data, 2019. Retrieved May 3, 2019 from: http://www.doitpom.ac.uk/tlplib/xr...ction/peak
5. Götze J. Chemistry, Texture and Physical Properties of Quartz – Geological Interpretation and Applications. Mineralogical Magazine. 2009; 73(4):645-671.
6. Götze J, Mökel R. Mineralogy, Geo-chemistry and Cathode Luminescence of Authigenic Quartz from Different Sedimentary Rocks. Quartz: Deposits, Mineralogy and Analytics. Springer, Berlin - Heidelberg, 2012, 287-306.
7. Hernandez MJ, Muñoz NA, Garcìa-Ruìz JP, Torres CV, Martin-Palma RJ, Manso SM. Nanostructured Porous Silicon: The Winding Road from Photonics to Cell Scaffolds; A Review, Frontiers in Bioengineering and Biotechnology. 2015; 3:1-60.
8. Hong Z, Liu A, Chen X, Jing XJ. Preparation of Bioactive Glass Ceramic Nanoparticles by Combination of Sol - gel and Co-precipitation Method. Journal of Non- Crystalline Solids. 2009; 355(6):368-372.
9. Lűhrs AK, Geurtsen W. The Application of Silicon and Silicates in Dentistry: A Review. Biosilica in Evolution, Morphogenesis and Nanotechnology. Springer, Berlin - Heidelberg, 2009, 359-380.
10. Meftah N, Mahbouh MS. Spectroscopic Characterization of Sand Dunes Minerals of El - Oued (Northeast Algerian Sahara) by FT–IR, XRF and XRD. Springer, Silicon. 2019; 12(3):1-7.
11. Moore P. High-Purity Quartz. Journal of Industrial Mineral. 2005; 8:54-57.
12. Muller A, Ihlen PM. Chemical Signature of Quartz and Feldspar in Polygeneration Pegmatites in Froland, Norway. Granitic Pegmatites. Paper presented at the State of Art International Symposium, Porto, Portugal, 2007. Retrieved March 28, 2007 from www.fc.up.pt/peg2007/files/muller.pdf
13. Nigerian Institute of Mining and Geosciences- NIMG. Laboratory Manual on Rocks and Minerals Analyses (Rev. Ed.). Mindiver, 2020, 317-335.
14. Obiefuna GI, Sini PH, Maunde A. Geochemical and Mineralogical Composition of Granitic Rock Deposits of Michika Area, Northeastern Nigeria. International Journal of Scientific and Technology Research. 2018; 7(4):160-170.
15. Roper DC, Hoard RJ, Speakman MD, Glascock, Cobry DA. Source Analysis of Central Plains Tradition Pottery using Neutron Activation Analysis: Feasibility and First Results. Plains Anthropologist. 2007; 53(203):325-335.
16. Sabri MM. Chemical and Structural Analysis of Rocks using X-Ray Fluorescence and X-Ray Diffraction

Techniques. The Scientific Journal of Koya University. 2020; 8(1):79-87.
17. Saikia BJ, Parthasarathy G, Sarmah NC, Baruah GD. Fourier Transform Infrared Spectroscopic Characterization of Naturally Occurring Glassy Fulgurites. Bulletin of Material Science. 2008a; 31:155-158.
18. Saikia BJ, Parthasarathy G, Sarmah NC. Fourier Transform Infrared Spectroscopic Estimation of SiO_2 based Rocks. Bulletin of Material Science. 2008b; 31:775-779.
19. Teji M, Kenichi M, Norimasa T, Nobuhiro I. Relationship among Quartz Crystallinity index, Grain size of Quartz and Conodont color Alteration index of Bedded Cherts in the Tamba belt, Southwest Japan. Journal of Geological Society. 2002; 108(12):806-812.